

Possibility of a New Ferroelectric Relaxor in the Layered Magnetic Insulator $[(\text{CH}_2)_3(\text{NH}_3)_2\text{Cu}_{1-x}\text{Cd}_x\text{Cl}_4]$, $x = 0, 0.3, 0.6,$ and 1

Mohga F. Mostafa, Ahmed A. Youssef, and Shaima S. Khaimy

Physics Department, Faculty of Science, University of Cairo, Cairo, Egypt

Reprint requests to M. F. M.; E-mail: mohga40@yahoo.com

Z. Naturforsch. **60a**, 507–511 (2005); received March 7, 2005

The dielectric permittivity of the layered magnetic insulators $[(\text{CH}_2)_3(\text{NH}_3)_2\text{Cu}_{1-x}\text{Cd}_x\text{Cl}_4]$ with $x = 0, 0.3, 0.6,$ and 1 has been studied in the temperature range 300 K–470 K at different frequencies. Single crystal- and powder-measurements for $x = 0$ revealed a ferroelectric phase transition at (434 ± 2) K. The ferroelectric Cu crystal and the antiferroelectric Cd salt were found to form solid solutions in the range $0.3 < x < 0.6$. The permittivity results of samples with $x = 0.3$ and 0.6 showed the broad permittivity-temperature plateau typical of dielectric relaxors. The two samples follow the relationship $1/\epsilon - 1/\epsilon_m = (T - T_m)^\gamma/C$, with $\gamma = 1.75$ and 1.71 and $C = 4.13 \cdot 10^5$ K and $1.19 \cdot 10^5$ K for $x = 0.3$ and $x = 0.6$ samples, respectively. Anomalous change in the temperature variation of the permittivity ($\delta\epsilon'/\delta T$) for the $x = 1$ sample at $T \sim 374$ K is ascribed to a structural phase transition. Thermal analysis for the $x = 0$ sample reveals two phase changes at $T_1 = 434.4$ K and $T_2 = 334.5$ K. The T_1 transition confirms the ferroelectric transformation, and the transition at T_2 is related to an order-disorder phase change. — PACS #:81.05.-t, 77.22.-d

Key words: Ferroelectrics; Dielectric Response; Relaxors.

1. Introduction

The copper and cadmium complexes $[(\text{CH}_2)_3(\text{NH}_3)_2\text{CuCl}_4]$ and $[(\text{CH}_2)_3(\text{NH}_3)_2\text{CdCl}_4]$ are members of the alkylene diammonium perovskite family. Single crystal X-ray investigations at room temperature have indicated that the two materials crystallize in the orthorhombic space group $Pmna$ [1, 2]. The structure consists of metal chloride octahedra and sharing corners forming two-dimensional layers. In the copper sample, the $[\text{CuCl}_6]^{2-}$ octahedra are tetragonally distorted with two short Cu,Cl bond distances of 2.275(4) Å and two long Cu,Cl distances of 2.946(4) Å. Two Cu,Cl bonds are nearly perpendicular to the layer with distances of 2.314(4) Å and a Cu-Cl-Cu bridging angle of 165.7(4)°. The chlorocuprate sheet is puckered as a result of the hydrogen bonding to the propylene-1,3-diammonium ion which lies between the layers. The cadmium sample has equal bridging Cd,Cl distances (Cd,Cl = 2.67 Å) with the bridging Cd-Cl-Cd angle 160.8° and two short terminal Cd,Cl distances of 2.58 Å. The organic cation is ordered and planar. The lattice parameters of both materials are listed in Table 1. The cadmium compound is known to undergo a phase transformation from an antiferrodistortive phase ($Pmna$) to a high tempera-

ture dynamically disordered paraelectric phase ($Imma$) at 375 K, with permanent dipoles lying in the trans-planes on chains parallel to the layers. The ordering of the chains leads to a planewise antiparallel polarized structure [3]. To the best of our knowledge no reports on the dielectric properties of the copper salt have been published. Also, since the two materials have the same crystalline structure at room temperature and are composed of the same cation $[(\text{CH}_2)_3(\text{NH}_3)_2]^{2+}$ and the similar anions $[\text{CuCl}_6]^{2-}$ and $[\text{CdCl}_6]^{2-}$, there is a high possibility that they form solid solutions. The solid solution will experience frustration and possibly would realize a ferroelectric relaxor or a dipolar glass state [4]. It is the aim of the present work to investigate the phase transition and the dielectric property of the copper salt and solid solutions of the Cu-Cd system in the temperature range 300–450 K at different frequencies.

2. Experimental

2.1. Sample Preparation

The compounds were prepared as described in [5]. The results of the chemical analysis indicated the formation of the compounds $[(\text{CH}_2)_3(\text{NH}_3)_2\text{Cu}_{1-x}$

Lattice x	a Å	b Å	c Å	Terminal Å	Bridging (1) Å	Bridging (2) Å	Cd-Cl-Cd angle °	Space group	Ref.
1	7.373(5)	7.523(5)	19.111(8)	2.58	2.67		160.80	<i>Pmna</i>	[2]
0	7.200(2)	18.246(6)	7.451(2)	2.314	2.275	2.946	165.70(4)	<i>Pmma</i>	[1]

Table 1. Room temperature lattice parameters of $[(\text{CH}_2)_3(\text{NH}_3)_2\text{Cu}_{1-x}\text{Cd}_x\text{Cl}_4]$, $x = 0$ and 1.

Table 2. IR bands (in cm^{-1}) and assignment for $[(\text{CH}_2)_3(\text{NH}_3)_2\text{Cu}_{1-x}\text{Cd}_x\text{Cl}_4]$, $x = 0, 0.3, 0.6,$ and 1.

$(\text{CH}_2)_3(\text{NH}_3)_2\text{Cl}_2$	Cu	Cu0.7	Cu0.4	Cd	Assignment
1599, 1465	1583	1582	1582	1587	N-H def.
1407–1187	1487	1486	1486	1490	CH_2 wagg. / $(\text{NH}_3)^+$ / C-H str.
943	939	938	935	935	CH_2 rocking
	278,	291,	287,	248,	
	235	267	278	223	

$\text{Cd}_x\text{Cl}_4]$, where $x = 0, 0.31, 0.605,$ and 1, henceforth denoted as Cu, Cu0.7, Cu0.4 and Cd, respectively.

2.2. Dielectric Permittivity Measurements

The complex dielectric permittivity ϵ^* in the frequency range 60 Hz – 100 kHz was measured using a computer controlled lock-in amplifier, type PAR 5207. The temperature was measured using a copper constantan thermocouple. To ensure good electrical contact, each sample was coated with silver paste. The measuring technique and precautions to avoid stray capacitance are discussed in [6].

3. Results and Discussion

3.1. Infrared Spectra

The IR spectra obtained were typical for these alkylene-diammonim perovskites [7–9]. Table 2 lists the most characteristic absorption peaks and their assignment. The bands in the range $400\text{--}200\text{ cm}^{-1}$ are typical for M-Cl vibration [9]. It is evident that the replacement of Cd for Cu causes a shift in the M-Cl vibrations to lower wavenumbers, as expected. The IR and chemical analysis results confirm the formation of the newly prepared materials.

3.2. Differential Thermal Analysis (DSC)

Figure 1 shows the DSC thermograph for Cu using a Shimadzu (50)-differential scanning analyzer with a scanning speed of $10\text{ }^\circ\text{C}/\text{min}$. Two endothermic peaks are found at $T_1 = 434.4\text{ K}$ and $T_2 = 334.5\text{ K}$. Peak T_1 is very broad and of smaller entropy. Peak T_2 has a λ -like shape with a tail on the high temperature side.

Table 3. Thermodynamic parameters for $[(\text{CH}_2)_3(\text{NH}_3)_2\text{Cu}_{1-x}\text{Cd}_x\text{Cl}_4]$, $x = 0$ and 1.

Material	T_{peak}	ΔH J/mol	ΔS J/k-mol	Reference
Cu	434.4	661.525	1.53	this work
Cu	334.5	1272.4	3.7	this work
Cd	373	1805	4.85	[10]

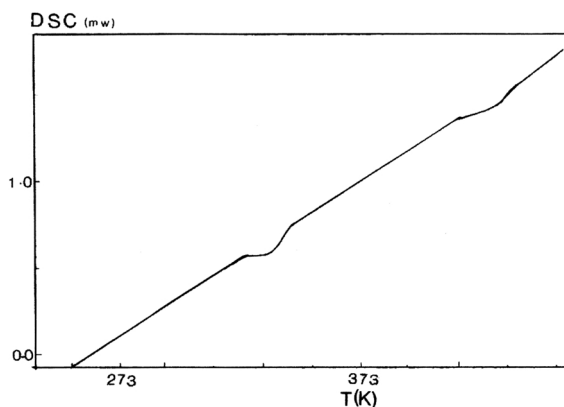


Fig. 1. Differential scanning thermograph of $[(\text{CH}_2)_3(\text{NH}_3)_2\text{CuCl}_4]$.

The large entropy of peak T_2 suggests an order-disorder phase transformation. The transition temperatures, enthalpies and entropies are listed in Table 3 along with the DSC results of the Cd as reported by Tello *et al.* [10].

3.3. Dielectric Permittivity

Figure 2a illustrates the real part of the dielectric permittivity as $\ln \epsilon'$ vs. temperature for Cu single crystal along the c -axis at the frequencies 60, 80, and 110 Hz. A sharp increase with a maximum at $T_1 \simeq 435\text{ K}$ is observed. The maximum decreases in height with increasing frequency, indicating a ferroelectric-like behavior. The increase in ϵ' for $T > 445\text{ K}$ is likely due to space charge polarization. The large increase in ϵ' at 435 K masks the presence of a permittivity plateau which is indicated by the arrow. The insert (Fig. 2b) shows the real part of the permittivity for the compressed pellet sample at 60 Hz, 410 Hz, and 2.01 kHz. The results show the ferroelectric transition superimposed over a permittivity plateau. The permittivity value in the plateau region decreases with

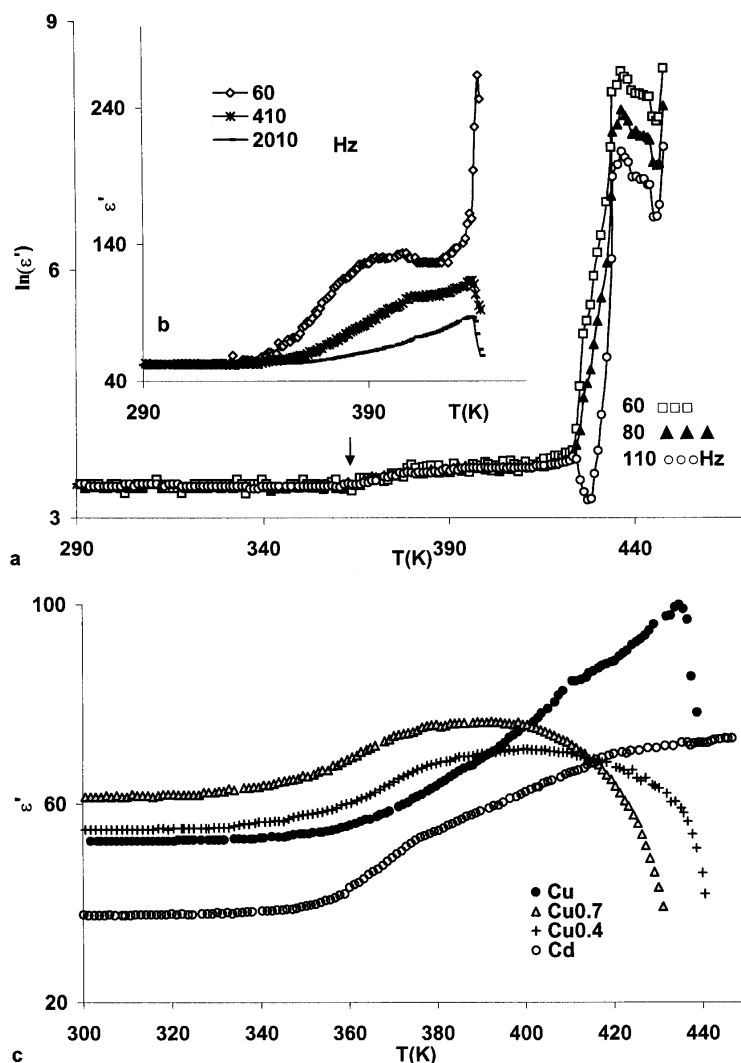


Fig. 2. a) Dielectric permittivity of $[(\text{CH}_2)_3(\text{NH}_3)_2\text{CuCl}_4]$ single crystal along c -direction. b) Dielectric permittivity of $[(\text{CH}_2)_3(\text{NH}_3)_2\text{CuCl}_4]$ powdered sample. c) Dielectric permittivity of powdered $[(\text{CH}_2)_3(\text{NH}_3)_2\text{Cu}_{1-x}\text{Cd}_x\text{Cl}_4]$, $x = 0, 0.3, 0.6, \text{ and } 1$ at 1.01 kHz.

increasing frequency. This behavior is typical of rotational dipoles [11, 12]. At $T < 360$ K a frequency and temperature-independent behavior prevails. Figure 2c shows the permittivity-temperature relation for Cu, Cu0.7, Cu0.4 and Cd samples at 1.01 kHz. In the low temperature range $T < 360$ K the permittivity of all samples is temperature-independent. However, as temperature increases, the permittivity of samples Cu0.7 and Cu0.4 increases gradually, resulting in peaks with broad maxima. In contrast to the Cu0.7 and Cu0.4 permittivity temperature behavior, the permittivity of the Cd sample increases gradually, reaching a plateau typical of dipole rotation [11, 12]. A change in the rate of increase of ϵ' is observed at 374 K which reflects the

phase transformation reported by Tello *et al.* [10] and by Kind *et al.* [3].

Figure 3a shows the effect of frequency on the temperature dependence of the permittivity for the Cu0.7 sample. The maxima T_m of the peak shift to higher temperature with increasing frequency in a manner similar to diffuse ferroelectric behavior [13–15]. A strong dispersion at $T < T_m$ and a weak dispersion at $T > T_m$ is noted. Another important feature in ϵ' is the shift of the broad plateau to higher temperature with increasing percentage of Cd content, see Figure 2c.

In order to characterize the dielectric dispersion and differences of the doped samples we used the empirical

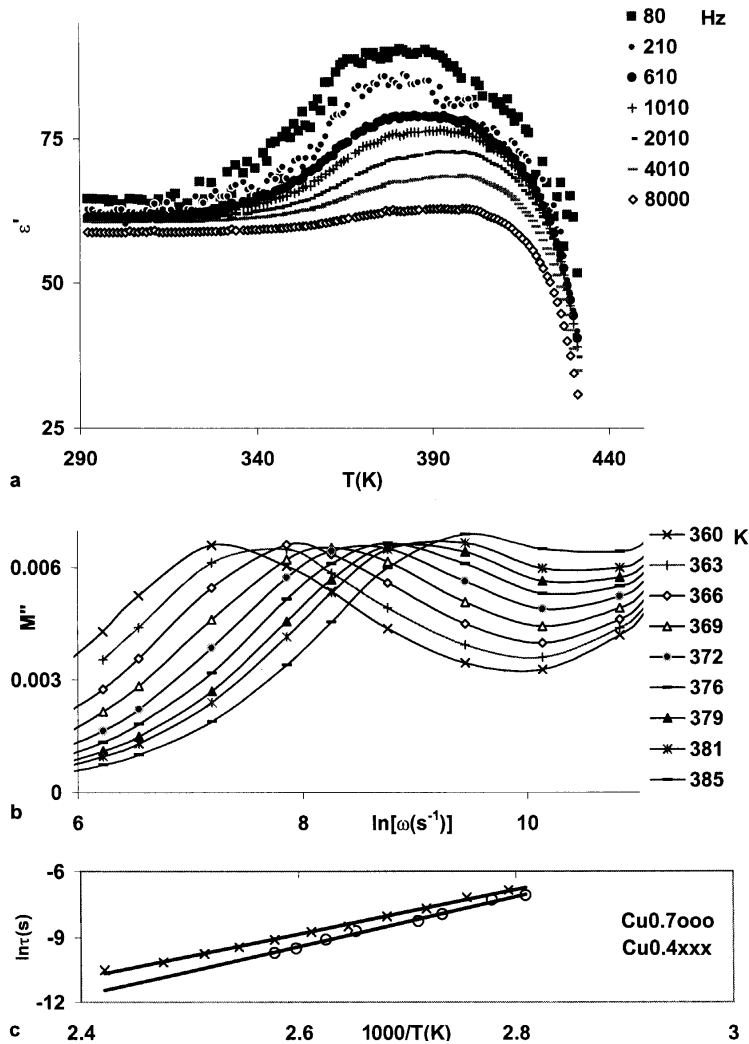


Fig. 3 a) Dielectric permittivity of powdered $[(\text{CH}_2)_3(\text{NH}_3)_2\text{Cu}_{0.7}\text{Cd}_{0.3}\text{Cl}_4]$ at selected frequencies. b) M'' vs. $\ln[\omega(\text{s}^{-1})]$ for the Cu0.7 sample at selected temperatures. c) Relaxation time vs. reciprocal temperature $[1000/T(\text{K})]$ for Cu0.7 and Cu0.4 samples.

expression [16, 17]

$$1/\epsilon - 1/\epsilon_m = (T - T_m)^\gamma / C. \quad (1)$$

γ and C are constants, where $1 \leq \gamma \leq 2$. $\gamma = 1$ holds for normal ferroelectrics and $\gamma = 2$ for an ideal relaxor. C is the Curie constant. Values of γ and C are 1.75 and $4.13 \cdot 10^5$ K and 1.71 and $1.19 \cdot 10^5$ K for Cu0.7 and Cu0.4 samples, respectively. The degree of relaxation behavior can be described by the parameter $\Delta T_{\text{relaxor}}$, which is given by [16, 17]

$$\Delta T_{\text{relaxor}} = T_{m(80 \text{ kHz})} - T_{m(80 \text{ Hz})}. \quad (2)$$

$\Delta T_{\text{relaxor}}$ was found to be 6.2 K and 8.1 K for Cu0.7 and Cu0.4, respectively.

The conductivity relaxation model, in which the dielectric modulus is defined as $M^* = 1/\epsilon^*$, can be used to get information about the relaxation mechanism in the absence of a well-defined dielectric loss peak [18]. Figure 3b shows the frequency spectra of $M''(\omega)$ at different temperatures for the Cu0.7 sample. The bell shaped peak shifts to higher frequencies with increasing temperature. The frequency ω_c , at which the maximum of $M''(M''_{\text{max}})$ occurs, defines the relaxation time τ_c by

$$\omega_c \tau_c = 1. \quad (3)$$

The temperature and frequency dependence of $M''(\omega)$ for the other samples shows similar results, except the difference in their magnitudes. The relaxation

time obtained from (3) yields a relaxation time in the range 10^{-5} s for Cu_{0.7} and Cu_{0.4}, which cannot be attributed to elementary dipoles. The large relaxation time indicates that the Debye-type relaxation is associated with the relaxation of clusters of dipoles. A plot of the relaxation times vs. temperature is depicted in Figure 3b. It reveals a thermally activated behavior following the Arrhenius relation

$$\tau = \tau_0 \exp(\Delta E/kT). \quad (4)$$

τ_0 is the high temperature limit of the relaxation time and ΔE the energy barrier. Least squares fitting to (4) yields $\Delta E = 0.97$ and 0.86 eV and $\tau_0 = 1.24 \cdot 10^{-17}$ and $6.31 \cdot 10^{-16}$ s for Cu_{0.7} and Cu_{0.4}, respectively.

A spread of the transition temperature over a wide range has been observed for many ferroelectric relaxors [19, 20]. This is attributed to differences in i) compositional fluctuations and ii) structural disorder, that probably results from symmetry differences of the metal halide octahedra [19, 20].

The latter can be related to the difference in the ionic size of the two ions. The Cu²⁺ ion is smaller than the Cd²⁺ ion [$r(\text{Cu}^{2+})/r(\text{Cd}^{2+}) = 0.74$]. Therefore replacement of Cu²⁺ by Cd²⁺ leads to off center Cd²⁺ ions and hence the formation of dipoles. It is known that

in ferroelectric relaxors only micropolar clusters and no macrodomains exist [21, 22]. Based on this fact it is reasonable to assume that the dipoles formed by the off center Cd²⁺ ions behave as non-interacting dipoles at low concentration of Cd. Addition Cd²⁺ intervenes with the long range ordering of the ferroelectric interaction, leading to the diffuse ferroelectric characteristic for solid solutions in the range $0.4 < x < 0.7$.

4. Conclusion

DSC and permittivity measurements of the layered magnetic insulator [(CH₂)₃(NH₃)₂CuCl₄] showed two phase transitions at $T_1 = (434 \pm 2)$ K and $T_2 = (334 \pm 1)$ K. The former is associated with a ferroelectric transformation, the latter with an order-disorder phase change. The mixed solid solution of Cu-Cd showed diffuse transitions which may be characterized as “ferroelectric relaxor” with the broad maximum that is a function of the frequency and concentration of the doping ion.

To the best of our knowledge this is the first report on relaxor type characteristics in layered magnetic insulators of the type [(CH₂)_{*n*}(NH₃)₂MCl₄], where M is a divalent transition metal ion. Detailed permittivity and transport properties will be published soon.

- [1] D. Pheps, D. Losee, W. Hatfield, and D. Dodgson, *Inorg. Chem.* **15**, 3147 (1976).
- [2] R. D. Willett, *Acta Cryst.* **B33**, 1641 (1977).
- [3] R. Kind, S. Plesko, and J. Roos, *Phys. Status Solidi A* **47**, 233 (1978).
- [4] B. Vugmeister and M. Glinchulk, *Rev. Modern Phys.* **62**, 993 (1990).
- [5] M. F. Mostafa, A. A. A. Youssef, and S. S. El-Hakim, *Phase Transitions* **77**, 317 (2004).
- [6] M. F. Mostafa, M. M. Abdel-Kadar, A. S. Atallah, and M. El-Nimer, *Phys. Status Solidi A* **135**, 549 (1993).
- [7] S. Kararup and R. Burg, *J. Sol. Stat. Chem.* **26**, 59 (1978).
- [8] S. Kammoun and A. Daoud, *Phys. Status Solidi* **162**, 575 (1997).
- [9] G. Snyder, *Mol. Spectrosc.* **4**, 411 (1990).
- [10] M. Tello, M. Ariendiaga, and J. Fernandez, *Solid State Comm.* **24**, 299 (1977).
- [11] R. Jakubas, G. Bator, M. Foulon, J. LeFebver, and J. Matuszewski, *Z. Naturforsch.* **48a**, 529 (1992).
- [12] M. F. Mostafa, A. A. A. Youssef, *Z. Naturforsch.* **56a**, 568 (2001).
- [13] A. P. Levanyuk, A. S. Sigov, and A. A. Sobyonin, *Zh. Eksp. Teor. Fiz.* **76**, 345 (1979). [*Sov. Phys. (JETP)*. **49**, 176 (1979).]
- [14] A. Glazounov, A. Bell, and A. Tagantsev, *J. Phys.: Condens. Matter* **7**, 4145 (1995).
- [15] U. Hochli, H. Weickel, and L. A. Boatner, *Phys. Rev. Lett.* **39**, 1158 (1976).
- [16] K. Uchino and S. Nomura, *Ferroelectr. Lett. Ect.* **4**, 55 (1982).
- [17] A. Tavernor and N. Thomas, *J. Eur. Cerm. Soc.* **13**, 121 (1993).
- [18] P. B. Macedo, C. T. Moynihan, and R. Bose, *Phys. Chem. Glasses* **13**, 171 (1972).
- [19] Z. Ban, S. Alpay, and J. Mantese, *Integrated Ferroelectric* **58**, 1281 (2003).
- [20] A. A. Bokov and Z. G. Ye, *J. Phys.: Condens. Matter* **1**, L541 (2000).
- [21] M. Tyunina and J. Levoska, *Phys. Rev.* **B65**, 132101 (2000).
- [22] C. Ang and Z. Yu, *J. Appl. Phys.* **91**, 1487 (2002).